# The Role of the Protein Core in the Inhibitory Power of the Classic Serine Protease Inhibitor, Chymotrypsin Inhibitor 2†

Evette S. Radisky,‡ David S. King,‡,§ Gene Kwan,‡,⊥ and Daniel E. Koshland, Jr.*,‡

*Department of Molecular and Cell Biology and Howard Hughes Medical Institute, University of California, Berkeley, California 94720*

*Received February 18, 2003*

ABSTRACT: A synthetic cyclic peptide, reported to be a tight-binding inhibitor of serine proteases, is instead found to be a good substrate, as is the linear peptide of the same sequence. Both of the peptides, designed to mimic the binding loop of chymotrypsin inhibitor 2 (CI2), were cleaved by subtilisin primarily at the CI2 reactive-site Met-59−Glu-60 bond, revealing that the sequence, in the absence of the structural context of the inhibitor, provides sufficient specificity for hydrolysis of this bond. Insights from the crystal structure of the CI2/subtilisin complex, together with biochemical analysis of a CI2 Gly-83 deletion mutant, have allowed us to identify key features that make CI2 an effective inhibitor, while the cyclic and linear peptides are substrates.

The protein inhibitors of serine proteases present a curious anomaly. They form phenomenally tight complexes with their target enzymes, exhibiting $K_i$ values as low as $10^{-14}$ M, and although they bind to proteases in a substrate-like manner, they undergo cleavage only very slowly, if at all (*1*, *2*). Chymotrypsin inhibitor 2 (CI2),[1] a protein of 83 amino acids, is a classic example of these inhibitors (*3*−*5*). For the complex formed between CI2 and subtilisin, we have recently shed some light on this mystery, showing that formation of an acyl−enzyme intermediate (the first chemical step in catalysis) occurs rapidly but is followed by an enormous delay in the subsequent deacylation step (*6*). It appears that the cleaved peptide product formed in the acylation step is retained in the active site of the enzyme, oriented to inhibit the hydrolysis reaction and favor religation of the peptide bond.

The structure of CI2 in complex with subtilisin suggests reasons for this behavior (*6*; Figure 1A). The binding loop of the inhibitor (residues 54−63) is stabilized by an extensive intramolecular hydrogen-bonding network involving CI2 residues Thr-58, Glu-60, Arg-62, Arg-65, Arg-67, and Gly-83. The loop is tethered at either end to the $\beta$-sheet of the hydrophobic protein core, and the Arg-65 and Arg-67 side chains extend from the $\beta$-sheet to hydrogen bond with the binding loop on either side of the scissile peptide bond (Met-59−Glu-60). Scrutiny of the CI2 structure reveals that all of the hydrogen-bonding residues of this network, with the exception of the C-terminal Gly-83, lie within a contiguous stretch of primary sequence (residues 53−70), forming a circular topology (Figure 1B). It therefore seems possible that a cyclic peptide incorporating these residues might partially recapitulate the inhibitory structure and function of CI2. Leatherbarrow and Salacinski reported that such a peptide, cyclized through an engineered disulfide bond (Figure 1C), inhibits several enzymes, including subtilisin, with affinity indistinguishable from that of intact CI2, and with no evidence for vulnerability to cleavage (*7*).

Since the cyclic peptide described by Leatherbarrow and Salacinski lacks the three Gly-83 hydrogen bonds, as well as any conformational stability conferred by the $\beta$-sheet itself, the inhibitory activity and resistance to proteolysis of the peptide should provide information on the functional importance of these features. To investigate the structural determinants of inhibition in greater detail, we carried out studies comparing the inhibitory and substrate properties of the 18-amino acid linear and cyclized peptides, CI2, and a CI2 Gly-83 deletion mutant (G83Δ-CI2). Comparison of the differential binding and hydrolysis of these species by subtilisin allows us to propose a more exact model for the structural basis of CI2 inhibition that provides insight into general principles governing inhibitor stability.

## EXPERIMENTAL PROCEDURES

*Subtilisin BPN′.* Recombinant subtilisin BPN′ (*8*), modified by the addition of a C-terminal 6-His tag (*6*), was prepared

† This work was supported in part by National Institutes of Health Grant DK09765 (to D.E.K.). E.S.R. was supported by a National Institutes of Health postdoctoral fellowship.

* To whom correspondence should be addressed. E-mail: dek@uclink.berkeley.edu.

‡ Department of Molecular and Cell Biology.

§ Howard Hughes Medical Institute.

⊥ Present address: UCSD School of Medicine, La Jolla, CA 92093.

[1] Abbreviations: CI2, chymotrypsin inhibitor 2; G83Δ-CI2, CI2 Gly-83 deletion mutant; $OD_{500}$, optical density measured at 500 nm; Ni−NTA, nickel−nitrilotriacetic acid; SDS−PAGE, sodium dodecyl sulfate−polyacrylamide gel electrophoresis; MS, mass spectrometry; ESI, electrospray ionization; amu, atomic mass unit; suc-Ala-Ala-Pro-Phe-pNA, *N*-succinyl-Ala-Ala-Pro-Phe *p*-nitroanilide; FMOC, 9-fluorenylmethoxycarbonyl; DCC, *N*,*N*′-dicyclohexylcarbodiimide; HOBT, 1-hydroxybenzotriazole; TFA, trifluoroacetic acid; HPLC, high-pressure liquid chromatography; RP-HPLC, reversed-phase HPLC; FTICR, Fourier transform ion cyclotron resonance; ppm, parts per million; IPTG, isopropyl $\beta$-D-1-thiogalactopyranoside; BSA, bovine serum albumin; PCR, polymerase chain reaction; DTT, DL-dithiothreitol; DMSO, dimethyl sulfoxide; MALDI-TOF, matrix-assisted laser desorption/ionization time-of-flight; TCEP, tris(2-carboxyethyl)phosphine; *m*/*z*, mass-to-charge ratio; SEM, standard error measurement.

10.1021/bi034275d CCC: $25.00 
Published on Web 05/08/2003

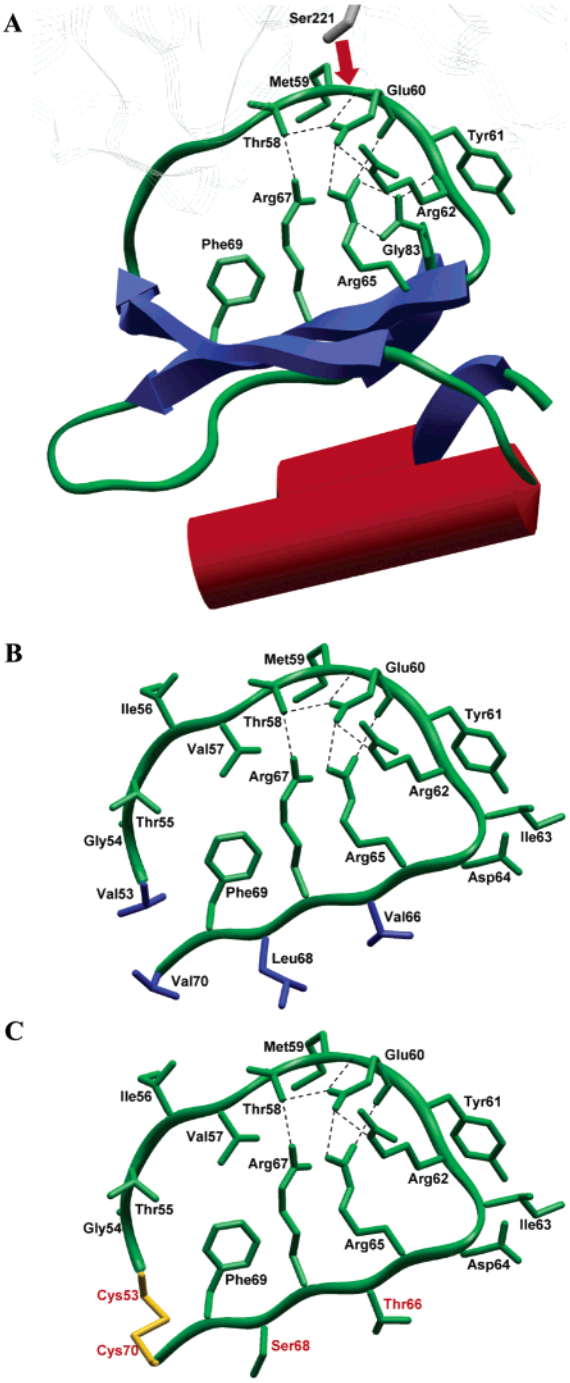


FIGURE 1: (A) Rendering of CI2 in complex with subtilisin, with coordinates from PDB 1LW6 (*6*). Helices are depicted in red and $\beta$-strands in blue. Side chains of residues potentially important in binding loop interactions with subtilisin or with the CI2 core are shown in green. Subtilisin is shown in light gray; the position of nucleophilic attack of subtilisin Ser-221 on the CI2 backbone, between Met-59 and Glu-60, is indicated with a red arrow. (B) The circular portion of the CI2 structure, including the binding loop and the third $\beta$-strand, on which the 18-amino acid cyclic peptide was based. Side chains shown in blue were mutated to alternative residues in the peptide: Val-53 and Val-70 were replaced with cysteine residues to allow disulfide cyclization, while Val-66 and Leu-68, originally sequestered in the hydrophobic core of the protein, were altered to threonine and serine, respectively, with the intention of promoting solubility and conformational stability. (C) A possible structure for the cyclic peptide, based on the structure of CI2. Note that of the nine H-bonds drawn in the CI2 structure, six potentially remain in the peptide, but the remaining three, in which Gly-83 served as a hydrogen acceptor, are no longer possible.

in protease-deficient *Bacillus subtilis* strain BG2036 (*9*). Because concatameric DNA is required for transformation of *B. subtilis*, the expression plasmid was prepared from *Escherichia coli* strain MM294, which produced 50% of the plasmid DNA in concatemeric form. *B. subtilis* strain BG2036 was grown to optimize transformation competency based on procedures developed by Bott and Wilson (*10*, *11*). Overnight cultures grown in LB media were harvested by centrifugation, resuspended in a minimal salts solution (1.4% $K_2HPO_4$, 0.6% $KH_2PO_4$, 0.2% $(NH_4)_2SO_4$, and 0.19% $Na_3$-Citrate·$2H_2O$), and then used to inoculate 100 mL of a synthetic medium containing 0.5% glucose, 1.4% $K_2HPO_4$, 0.6% $KH_2PO_4$, 0.2% $(NH_4)_2SO_4$, 0.19% $Na_3Citrate·2H_2O$, 0.072% $MgSO_4$, and 0.005% of each of the following amino acids: Trp, His, Arg, Val, Lys, Thr, Gly, Asp, and Met. Cultures were grown at 37 °C with shaking to an $OD_{500}$ of 0.5, and then for an additional 2−3 h before transformation. The expression plasmid was introduced into the competent cells by mixing 0.5−1 $\mu$g of DNA with 1 mL of culture and then incubating at 37 °C with shaking for 1 h. Transformations were plated onto LB agar supplemented with 12.5 $\mu$g/mL chloramphenicol.

Expression cultures were grown in 2× YT media, supplemented with 10 mM $CaCl_2$ and 12.5 $\mu$g/mL chloramphenicol, at 37 °C with shaking for 20−24 h. Cultures were clarified by centrifugation, and secreted mature subtilisin was recovered from the media by precipitation with 3 vol of 95% ethanol. The drained protein pellet from a 500-mL culture was redissolved in 80 mL of binding buffer containing 50 mM $KH_2PO_4$ (pH 6.5), 20 mM imidazole, and 300 mM NaCl; the solution was clarified by centrifugation, and 1.5 mL of Ni−NTA agarose slurry (Qiagen) was added. The solution was mixed at 4 °C on a rotary mixer for 3 h; the resin was then packed, washed with 40 mL of binding buffer, and eluted with 10 mL of elution buffer containing 50 mM $KH_2PO_4$ (pH 5.8), 250 mM imidazole, and 300 mM NaCl. Purified subtilisin was dialyzed into 10 mM $NH_4OAc$ (pH 5.8) and 5 mM $CaCl_2$ at 4 °C for 24 h and then lyophilized and stored at −80 °C until use. The purified enzyme appeared to be homogeneous by SDS−PAGE with Coomassie staining; the mass, verified by ESI-MS, was within 1 amu of the calculated molecular mass.

Initially, the active enzyme concentration was quantified by active-site titration using *N-trans*-cinnamoylimidazole (*12*, *13*). Titrated subtilisin was used in kinetic studies with the substrate suc-Ala-Ala-Pro-Phe-pNA (Sigma), where initial rates were determined from the absorbance increase caused by the release of *p*-nitroaniline ($\epsilon_{410} = 8480\ M^{-1}\ cm^{-1}$; *14*), and substrate concentrations were determined from the absorbance after total hydrolysis; a $K_M$ of 270 ± 10 $\mu$M and a $k_{cat}$ of 50 ± 2 $s^{-1}$ were observed. Subsequently, active enzyme concentrations were routinely measured by kinetic assay with suc-Ala-Ala-Pro-Phe-pNA.

*Synthetic Peptides.* Peptides were synthesized by FMOC chemistry (DCC/HOBT activation) on an ABI 431A synthesizer via user-devised cycles and were cleaved/deprotected with Reagent K. Essentially complete cyclization was achieved by dissolving reduced peptide at 1 mg/mL in water containing 50% 1-propanol and 0.4% DMSO. The solution was stirred open to the air; after 48 h, the 1-propanol had evaporated and the concentrated solution was acidified. The peptide was purified directly with an acetonitrile gradient in

water, both containing 0.1% TFA, on a Vydac 300-Å pore C18 reversed-phase column. Peptide purity and cyclization were monitored by RP-HPLC as well as by ESI−ion trap (Bruker Agilent) and ESI−FTICR (Bruker Apex III, 9.4-T magnet) MS. Both peptides were within 1 ppm of their calculated masses, with purity >96%.

*CI2.* The CI2 expression construct was created using pET27b(+) (Novagen) as previously described (*6*). Expression cultures in LB containing 15 μg/mL of kanamycin were innoculated with 0.1 vol of an overnight culture, incubated at 37 °C with shaking for 1 h, induced by the addition of IPTG to 0.5 mM, and incubated at 37 °C with shaking for an additional 4 h. Cells were recovered by centrifugation, washed with a volume of 0.15 M NaCl equivalent to 1/10 of the culture volume, repelleted, and frozen at −20 °C. Thawed cells were thoroughly resuspended in 10 mM Tris (pH 8.0) containing 2 mM EDTA, and then cell debris was removed by centrifugation. The periplasmic extract containing CI2 was acidified to pH 4.5 with HCl, and the precipitate formed was removed by centrifugation. The resultant supernatant was loaded onto SP Sepharose (Pharmacia) equilibrated with 20 mM NaOAc (pH 4.5); CI2 was eluted with a linear gradient from 0 to 1 M NaCl. Purified CI2 was subsequently dialyzed into 10 mM $NH_4OAc$ (pH 5.8), lyophilized, and stored at −80 °C until use. We routinely recovered 120−140 mg of pure CI2 per liter of culture; the protein appeared to be homogeneous by SDS−PAGE with Coomassie staining, and the mass determined by ESI-MS was within 1 amu of the calculated molecular mass.

CI2 concentrations were determined by titration with subtilisin of known concentration (*15*). Subtilisin was incubated for 15−30 min at room temperature with a range of substoichiometric concentrations of CI2 and then assayed for residual activity with the substrate suc-Ala-Ala-Pro-Phe-pNA as described above. A plot of residual enzyme activity vs CI2 concentration allowed extrapolation to the stoichiometric equivalence point. The active inhibitor concentrations thus obtained agreed well with total protein determinations by the Bradford method (*16*), using BSA as a standard.

CI2 refers here to recombinant CI2 lacking the first 19 (disordered) amino acids, with Leu-20 replaced by a new starting Met codon and additional substitutions Glu-45 → Ala and Lys-72 → Arg. The substituted residues, all at solvent-exposed positions, have no detectable effect on the backbone structure of CI2 (*6*). Furthermore, the binding constant for binding to subtilisin BPN′ that we obtain with this CI2 variant is identical to that reported for full-length, unsubstituted CI2 (*17*); we therefore consider the substitutions to be functionally silent. Throughout the text, we use the amino acid numbering corresponding to full-length CI2.

*G83Δ-CI2.* The CI2 expression construct was mutagenized using the PCR-based QuikChange method (Stratagene) to replace the codon for Gly-83 with a new TGA stop codon; the mutated construct was verified by DNA sequencing. The truncated mutant protein was expressed and purified following the same protocols used for CI2. Expression levels were poor by comparison with CI2, allowing purification of only 4 mg/L of culture; furthermore, the G83Δ-CI2 thus obtained was contaminated with an equivalent amount of another protein. G83Δ-CI2 was further purified to homogeneity by preparative-scale RP-HPLC on a 250- × 10-mm Vydac 300-Å pore C18 column prior to enzyme inhibition and hydrolysis studies; the correct molecular mass was verified by ESI-MS.

G83Δ-CI2 was not sufficiently resistant to subtilisin hydrolysis to allow concentration determination by enzyme titration. Instead, concentrations were routinely determined by peak integration from RP-HPLC absorbance traces monitored at 220 nm with a Shimadzu SPD-10A UV−vis detector and processed with Shimadzu EZChrom analysis software, using a calibration curve constructed with analytically pure CI2 of known concentration. The HPLC concentration determination method was highly reproducible and had the advantage that samples of variable purity could be accurately analyzed.

*Subtilisin Inhibition and Binding Studies.* Subtilisin assays were carried out at 25 °C in 0.1 M Tris (pH 8.6) with 1 mM DTT. In reactions in which the cyclic (oxidized) peptide was included as an inhibitor, DTT was omitted from the assay buffer. Stock solutions of the substrate suc-Ala-Ala-Pro-Phe-pNA were dissolved in 100% DMSO; the final assay composition after substrate addition included 4% DMSO. Up to seven 500-μL reactions were run simultaneously in glass cuvettes in a Hewlett-Packard HP8453 spectrophotometer equipped with a multicell transporter and a circulating waterbath.

For inhibitor titration studies, enzyme and inhibitor were preincubated at room temperature for 30−120 min at 25−100× their intended final concentrations; the reactions were then initiated by dilution of the enzyme/inhibitor mixture into pre-equilibrated cuvettes containing assay buffer and substrate. For the alternative substrate inhibition study, both substrate and inhibitor were added to assay buffer and equilibrated in cuvettes before the reactions were initiated by the addition of enzyme. In both types of experiment, the final enzyme concentration was typically 4−8 nM; reactions were rapidly mixed by inversion and then followed spectroscopically for 5 min to obtain initial rates. Data from the alternative substrate inhibition study were globally fitted by multiple regression to the competitive inhibition equation (see Results) using Tablecurve 3D (Jandel Scientific, San Rafael CA); all other linear and nonlinear regression analyses were carried out using Prism (GraphPad Software, San Diego CA).

Assay conditions and instrumentation for binding studies with CI2 and G83Δ-CI2 were identical to those employed in other subtilisin assays, except that the enzyme and inhibitor concentrations were much lower, and reactions were followed spectroscopically for 16 h rather than 5 min. Solutions of enzyme and inhibitor were prepared at 25× their intended final concentrations in 50 mM NaOAc (pH 6.0), 1 mM DTT, and 0.1 mg/mL BSA; inhibitor dilutions were prepared in parallel rather than serially to minimize losses caused by adhesion to plastic tubes. Reactions were initiated by the sequential addition of 20 μL each of inhibitor and enzyme solutions to reaction buffer containing substrate pre-equilibrated in cuvettes; the final enzyme concentration was typically 0.25 nM, while inhibitor concentration ranged from 3 to 15 nM for CI2, and from 10 to 200 nM for G83Δ-CI2. $K_i$ values reported represent mean values from duplicate experiments.

*Hydrolysis Studies.* The depletion of linear or cyclic peptide, CI2, or G83Δ-CI2 in time course incubations with subtilisin was monitored by HPLC. Reactions were carried out at 25 °C in 0.1 M Tris (pH 8.6) with 1 mM DTT; DTT

was omitted for the cyclic (oxidized) peptide reactions. Aliquots withdrawn at periodic intervals were quenched by acidification to pH 1 with HCl and frozen at −20 °C until analyzed. Samples were thawed, adjusted to 6 M urea, and injected onto a 50- × 4.6-mm Jupiter 5$\mu$ 300-Å column (Phenomenex). Enzyme, substrates, and hydrolysis products were resolved with an acetonitrile gradient (20−40% for linear and cyclic peptides, 35−50% for CI2 and G83Δ-CI2) in 0.1% TFA at a flow rate of 1 mL/min over 12 min. For each time point, HPLC injections were performed in duplicate. Remaining substrate quantities were determined by peak integration of absorbance traces monitored at 220 nm and comparison to standard curves generated from known quantities of pure linear peptide or CI2.

Reactions to be analyzed by MALDI-TOF mass spectrometry typically were run in 25 mM $NH_4HCO_3$ (pH 8.0), allowing immediate analysis without prior desalting. Aliquots were mixed 1:1 with a saturated solution of the matrix material α-cyano-3-hydroxycinnamic acid in acetonitrile/water containing 0.1% TFA, and the peptide masses were assessed with a Bruker Reflex III mass spectrometer in reflectron mode. Peaks were assigned to the appropriate peptide fragments with the help of the ExPASy FindPept tool (http://ca.expasy.org/tools/findpept.html; *18*). For the identification of primary cleavage sites in the cyclic peptide, the reaction mixture was separated on a 150- × 1.0-mm 5$\mu$ 300-Å Reliasil C18 column (Michrom Bioresources) with a 10−50% acetonitrile gradient in 0.083% TFA at a flow rate of 75 $\mu$L/min over 15 min. The isolated, singly cleaved product peptide was adjusted to neutral pH with $NH_4OH$, treated with a 4-fold excess of TCEP at 4 °C overnight, and then reanalyzed by MALDI-TOF MS. A portion of the reduced sample was adjusted to pH 9 with $NH_4OH$, treated with an excess of 4-vinylpyridine at 25 °C for 90 min, and again reanalyzed by MALDI-TOF MS.

## RESULTS

*Inhibition and Hydrolysis Studies with Synthetic Peptides.* The linear and disulfide cyclized peptides were initially tested for tight-binding inhibition by titration against subtilisin. On the basis of the previous report of Leatherbarrow and Salacinski (*7*), we expected to see nearly complete inhibition of the enzyme at stoichiometric concentrations of the cyclic peptide. Instead, we observed a lack of inhibition for both linear and cyclic peptides (Figure 2). Because our standard assay composition differed somewhat from that in the earlier report with respect to substrate and buffer concentrations and pH, we repeated the experiment precisely as previously described and again observed no inhibition. This result was reconfirmed when the titration was repeated at peptide concentrations extending to 10 000-fold excess over the enzyme concentration. To resolve the question of whether this lack of inhibition was due to (i) failure of the peptides to bind to subtilisin or (ii) rapid hydrolysis of the peptides by subtilisin during the preincubation period, we analyzed enzyme/peptide mixtures by mass spectrometry. No intact peptide was detected after a 15-min incubation in mixtures with a 100-fold excess of peptide, but various small hydrolysis products were observed.

As it was apparent that both the cyclic and linear peptides were clearly substrates for subtilisin, we investigated the

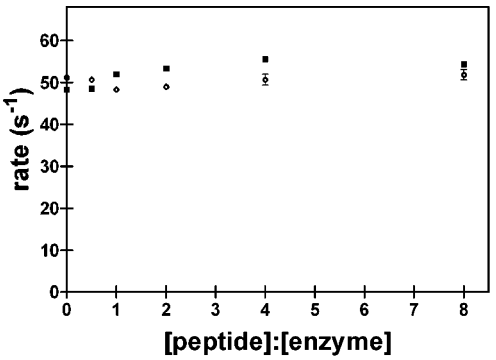


FIGURE 2: Lack of subtilisin inhibition by up to eight equivalents of linear or cyclic peptide. Filled squares represent linear (reduced) peptide, and open circles represent cyclic (oxidized) peptide; points are averages of duplicate assays, shown with bars representing the SEM. Subtilisin (0.7 $\mu$M) was preincubated with various stoichiometric ratios of linear or cyclic peptide for 2 h to allow complex formation, and then residual enzyme activity was assayed by 100× dilution of the enzyme/peptide mixture into assay buffer containing the substrate suc-Ala-Ala-Pro-Phe-pNA (1 mM).

kinetics of enzymatic peptide hydrolysis. The depletion of intact peptide over time was monitored by HPLC with a range of initial peptide concentrations and a catalytic concentration of enzyme. Initial rates were obtained from the progress curves by linear regression; a representative progress curve is shown in Figure 3A. For the linear peptide, the fit of the Michaelis−Menten equation to the initial rate data gave a $K_M$ of $1.9 \times 10^{-4}$ M and a $k_{cat}$ of 35 $s^{-1}$ (Figure 3B). For the cyclic peptide, the $k_{cat}$ of 2.6 $s^{-1}$ is well determined, but the $K_M$ of $7 \times 10^{-6}$ M is only an approximate value, because reactions with peptide concentrations below 5 $\mu$M fell beyond the sensitivity limits of the HPLC assay (Figure 3C).

Having shown that both peptides were rapidly hydrolyzed substrates of subtilisin, we anticipated that they should inhibit cleavage of a chromogenic substrate by subtilisin, not, as originally reported, as tight-binding inhibitors, but rather as competitive alternative substrates at higher concentrations. The rate equation for the reaction of one substrate in the presence of a competing substrate (considered for the moment to be the "inhibitor") takes the form of the classic competitive inhibition equation (eq 1), with the added condition that the observed $K_i$ for the "inhibitor" must be equivalent to its $K_M$ (*19*). An inhibition study following the

$$v = \frac{k_{cat}[E]_0[S]}{K_M(1 + [I]/K_i) + [S]} \quad (1)$$

hydrolysis of the substrate suc-Ala-Ala-Pro-Phe-pNA at varied concentrations of both substrate and the cyclic peptide confirmed our expectations; a double-reciprocal plot illustrates the characteristic effect of competitive inhibition (Figure 4). The $K_M$ and $k_{cat}$ values for the substrate, derived from a global fit of eq 1 to the inhibition data, were in excellent agreement with those determined in the absence of inhibitor, and the cyclic peptide $K_i$ of $2.5 \times 10^{-6}$ M was in fair agreement with the approximate $K_M$ reported above. Given the uncertainty inherent in the direct determination of $K_M$ for the cyclic peptide, we consider this $K_i$ value to be a more accurate estimation of $K_M$. Equivalent inhibition experiments were not carried out with the linear peptide, due to its lower affinity for subtilisin and limited solubility.

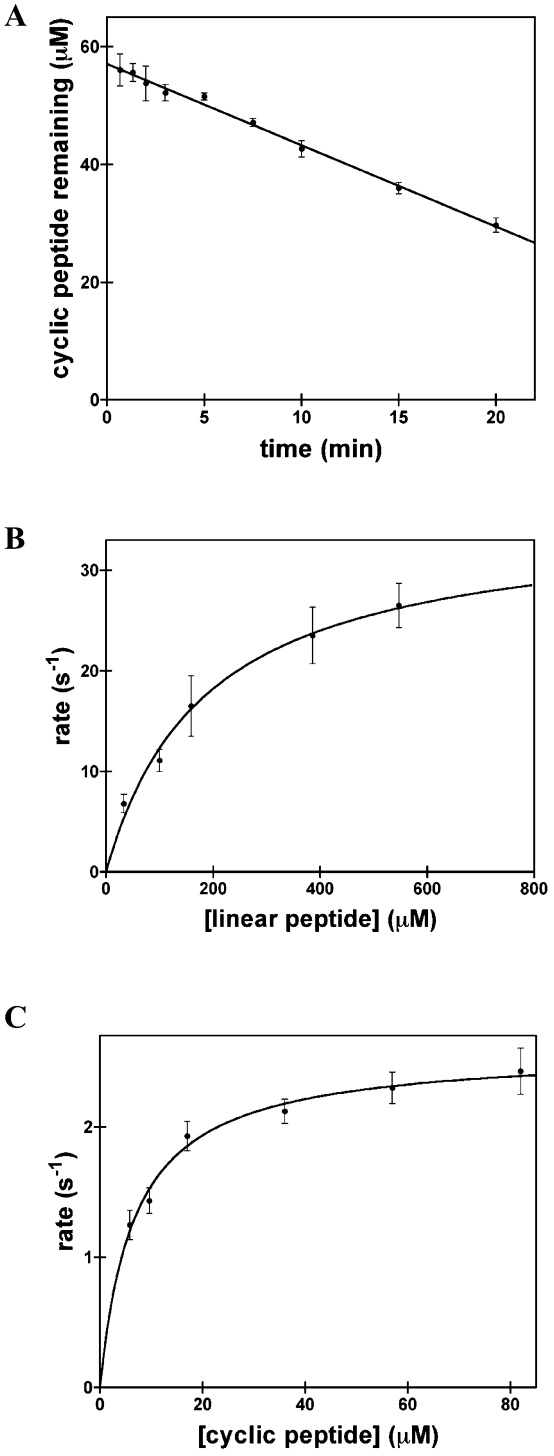


FIGURE 3: (A) Representative progress curve for peptide hydrolysis by subtilisin. The example shown is for a reaction with 57 $\mu$M cyclic peptide. Each point represents the averaged peptide peak area from duplicate HPLC injections, shown with bars representing the SEM. Fits of the Michaelis−Menten equation to plots of hydrolysis rate vs peptide concentration are shown for (B) the linear peptide and (C) the cyclic peptide. Each point represents a slope obtained by linear regression from a time course such as the one shown in (A); error bars represent the slope standard error.

The rapid hydrolysis of the linear and cyclic peptides could be interpreted as evidence that removal of the CI2 scaffold had severely compromised the proteolytic resistance of the original reactive-site bond (Met-59−Glu-60). However, a second possibility was that removal of the CI2 scaffold allowed the enzyme to bind the peptides in alternative

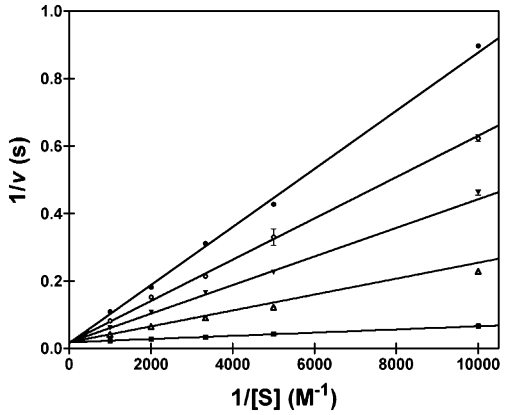


FIGURE 4: Data from a 5 × 5 inhibition study, displayed as a double-reciprocal plot of rate vs substrate concentration to illustrate the competitive nature of the inhibition. Linear fits (from top to bottom) represent 40, 30, 20, 10, and 0 $\mu$M cyclic peptide. Assays performed in duplicate contained, in addition to the cyclic peptide, 4 nM subtilisin and 1000, 500, 300, 200, or 100 $\mu$M suc-Ala-Ala-Pro-Phe-pNA.

binding modes, favoring alternative scissile peptide linkages. We addressed the question of cleavage site specificity for the synthetic peptides through an extensive mass spectrometric analysis of cleavage products from partial digests with subtilisin. From the variety of small fragments identified in longer digests, it was apparent that subtilisin is capable of cleaving the synthetic peptides at a multitude of sites, consistent with the well-recognized promiscuity of the enzyme (Figure 5A). However, we were particularly interested in identifying the site or sites of primary attack, differentiating the site of initial cleavage from secondary sites that are attacked only after an initial cleavage has already occurred.

In digests of the linear peptide that were quenched while a large proportion of the peptide was still intact, the only major product peak observed corresponded to the C-terminal fragment from cleavage at the Met-59−Glu-60 reactive-site bond (EYRIDRTRSFC, *m*/*z* 1445.7). Trace amounts of C-terminal fragments corresponding to cleavage at Tyr-61−Arg-62, Arg-62−Ile-63, and Asp-64−Arg-65 were also identified (RIDRTRSFC, *m*/*z* 1153.7; IDRTRSFC, *m*/*z* 997.5; RTRSFC, *m*/*z* 769.5) (Figure 5A). Each of these alternative cleavage products displayed less than 5% of the intensity of the major product peak. No N-terminal product peaks were identified, presumably because these much more hydrophobic fragments were not efficiently ionized; it is therefore impossible to know whether the minor product peaks represent secondary cleavage products or alternative sites of initial hydrolytic attack.

In determining the initial cleavage site(s) for the cyclic peptide, we could be more rigorous, thanks to the covalent disulfide linkage between the two fragments of the singly cleaved species. At early stages of digestion, the only product mass detected (*m*/*z* 2167) represented the intact peptide (*m*/*z* 2149) plus 18 amu from addition of the hydrolytic water molecule. HPLC separation of the reaction mixture yielded only three peptide peaks, representing the intact peptide, the singly cleaved product(s), and subtilisin. The product peak was isolated and the disulfide bond reduced; the products were then reanalyzed by mass spectrometry to determine the site(s) of cleavage. As we had observed for the linear peptide,

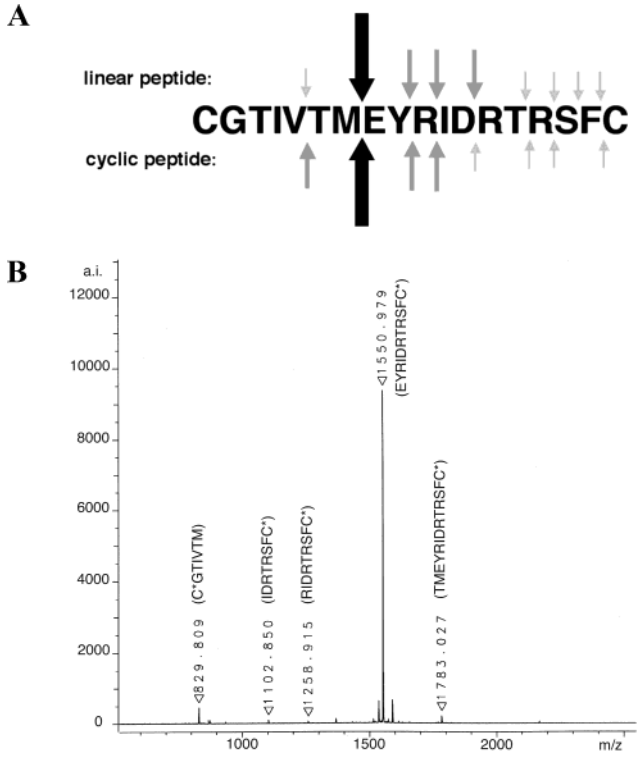


FIGURE 5: (A) Diagram showing the identified subtilisin cleavage sites in the synthetic peptide sequence. Heavy black arrows represent the major primary cleavage site for linear and cyclic peptides (Met-59−Glu-60 in both cases). Medium gray arrows indicate several alternative, less favored, primary cleavage sites, while small light gray arrows indicate secondary cleavages observed in further advanced digests. (B) Mass spectrum obtained from a sample of singly cleaved cyclic peptide, after HPLC purification, disulfide reduction, and cysteine derivatization with 4-vinylpyridine. Peaks corresponding to primary hydrolysis products are labeled with their respective sequences. C* represents vinylpyridine-modified cysteine.

the major product peak (>90%) was EYRIDRTRSFC (*m*/*z* 1445.7), confirming the reactive-site Met-59−Glu-60 bond as the major site of primary cleavage. Traces of TMEYRIDRTRSFC (*m*/*z* 1677.9), RIDRTRSFC (*m*/*z* 1153.7), and IDRTRSFC (*m*/*z* 997.5) were also observed, corresponding to alternative, less favored sites of primary cleavage at Val-57−Thr-58, Tyr-61−Arg-62, and Arg-62−Ile-63 (Figure 5A). As with the linear peptide, each of the alternative cleavage products displayed less than 5% of the intensity of the major product peak.

In an attempt to detect N-terminal cleavage products, the product peptide sample isolated above was derivatized with 4-vinylpyridine; it was hoped that this hydrophilic and readily protonated cysteine modification would improve the ability of the N-terminal fragments to form the gas-phase cations essential for detection by mass spectrometry. This strategy allowed detection of vinylpyridine-modified CGTIVTM (*m*/*z* 829.8), representing the N-terminal fragment from cleavage at the Met-59−Glu-60 reactive-site bond. While the peak for this modified N-terminal fragment was still much lower in intensity than that for the corresponding modified C-terminal fragment, it was of greater intensity than the peaks for the minor modified C-terminal fragments (Figure 5B). No N-terminal fragments from alternative primary cleavage sites were detected. Relative peak intensity in mass spectrometry is rarely a quantitative measure of relative concentration, because the observed intensity of a species depends heavily on the efficiency of gas-phase ionization. Nevertheless, taken in aggregate, the mass spectrometry results presented here strongly suggest that the reactive-site Met-59−Glu-60 bond in CI2 is also the most favored site of primary cleavage in both the linear and cyclic synthetic peptides.

*Inhibition and Hydrolysis Studies with CI2 and G83Δ-CI2.* Wild-type CI2 is a potent slow, tight-binding inhibitor of subtilisin, with an equilibrium dissociation constant ($K_i$) of $2.9 \times 10^{-12}$ (*17*). We confirmed this reported value for our recombinant variant and evaluated $K_i$ for the association of G83Δ-CI2 with subtilisin. Reactions with the chromogenic substrate suc-Ala-Ala-Pro-Phe-pNA in the presence of varying inhibitor concentrations were followed until steady-state rates were clearly reached. $K_{i(app)}$ and $K_i$ are described by eq 2, where $v_i$ and $v_0$ are the steady-state rates in the presence

$$K_{i(app)} = K_i(1 + [S_0]/K_M) = \frac{v_i/v_0}{(1 - v_i/v_0)}[I_0] - v_i/v_0[E_0] \quad (2)$$

and in the absence of inhibitor, $K_M$ is the Michaelis constant for subtilisin cleavage of suc-Ala-Ala-Pro-Phe-pNA, and $[I_0]$ and $[E_0]$ are the initial concentrations of inhibitor and enzyme (*20*). When inhibitor is in large excess over enzyme, as here, the enzyme concentration-dependent term is negligible, and eq 2 can be simplified and rearranged to eq 3, which predicts

$$(v_0 - v_i)/v_i = [I_0]/K_{i(app)} = [I_0]/K_i(1 + [S_0]/K_M) \quad (3)$$

that a plot of $(v_0 - v_i)/v_i$ vs $[I_0]$ will yield a straight line passing through the origin, with a slope of $1/K_{i(app)}$, allowing calculation of $K_i$ (*17*). CI2 displayed the expected slow, tight-binding behavior described previously. G83Δ-CI2, in contrast, displayed a pattern of "temporary inhibition" often seen with rapidly hydrolyzed inhibitors (*17*, *21*); over longer time courses, a slight upward curvature is observed in plots of absorbance vs time, as inhibitor is hydrolyzed and enzyme regains activity. Steady-state rates could still be obtained from the early stages of a time course, however. At the higher concentrations of inhibitor required with G83Δ-CI2, complex formation was rapidly achieved in the dead time while the reactions were prepared, and reliable steady-state rates were obtained from the initial 50 min of reaction (Figure 6A). When $(v_0 - v_i)/v_i$ was plotted vs $[I_0]$, the result was reasonably linear (Figure 6B), allowing calculation of a $K_i$ for G83Δ-CI2 of $3.4 \times 10^{-9}$ M, 3 orders of magnitude greater than the $K_i$ for CI2.

Initial steady-state rates for hydrolysis of CI2 and G83Δ-CI2 by subtilisin were measured using an HPLC assay similar to that employed with the linear and cyclic peptides. Although only a single initial concentration of CI2 and G83Δ-CI2 was tested, initial rates from the linear phase of the progress curves were expected to approximate $k_{cat}$ well, since CI2 and G83Δ-CI2 concentrations were at least 4 orders of magnitude greater than $K_i$, completely saturating the enzyme. The rate of CI2 hydrolysis was $3.8 \times 10^{-6}$ s$^{-1}$ (Figure 7A), while the rate of G83Δ-CI2 hydrolysis was increased by 3 orders of magnitude, $4.0 \times 10^{-3}$ s$^{-1}$ (Figure 7B).

## DISCUSSION

A comparison of the kinetic constants determined here with those previously reported for the cleavage of several

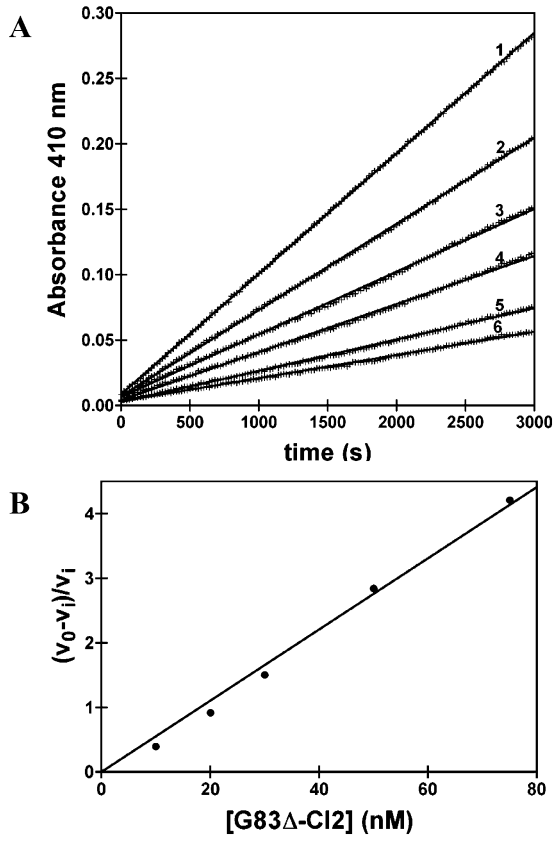


FIGURE 6: (A) Initial 50 min of a G83Δ-CI2 binding study. Fits by linear regression, approximating steady-state rates after equilibrium complex formation, are shown superimposed on the actual data points. Reactions 1−6, from top to bottom, contained 0, 10, 20, 30, 50, and 75 nM of G83Δ-CI2. In addition, each reaction contained 0.25 nM subtilisin and 1 mM suc-Ala-Ala-Pro-Phe-pNA. (B) Replot of the parameter $(v_0 - v_i)/v_i$ vs G83Δ-CI2 concentration. The slope of the fitted line, constrained to pass through the origin, was used to calculate $K_i$ using eq 3.

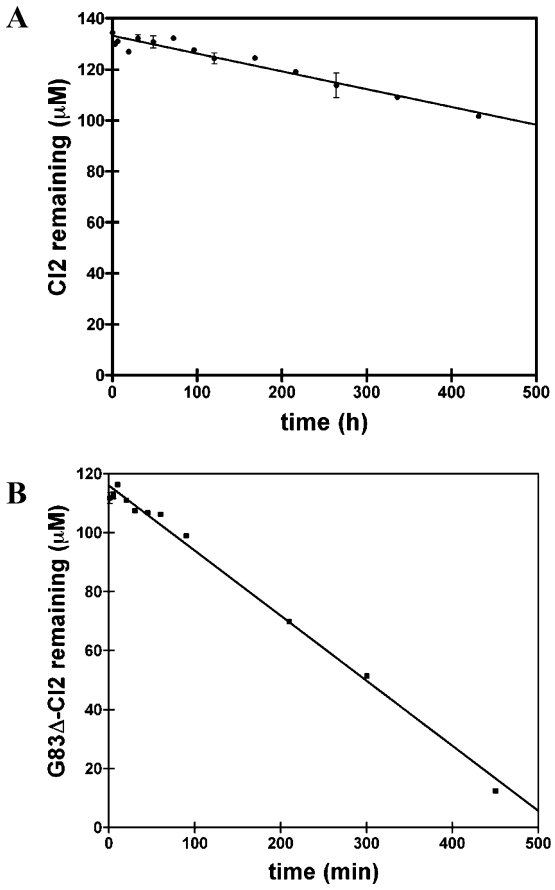


FIGURE 7: Hydrolysis time courses for (A) CI2 and (B) G83Δ-CI2. The CI2 reaction contained 133 $\mu$M CI2 and 5 $\mu$M subtilisin, while the G83Δ-CI2 reaction contained 116 $\mu$M G83Δ-CI2 and 0.9 $\mu$M subtilisin. Note the different time scales of the two reactions. Despite containing a lower enzyme concentration, the G83Δ-CI2 reaction is nearly depleted of intact inhibitor after 450 min, whereas in the CI2 reaction, most inhibitor is still intact after 432 h.

classes of good substrates by subtilisin is shown in Table 1. Substrates chosen for this comparison possess a favorable residue (usually Phe) at the $P_1$ primary specificity subsite and fill many of the subsites in the subtilisin binding cleft. The chromogenic substrate suc-Ala-Ala-Pro-Met-pNA features a Met residue at the $P_1$ position as found in CI2; this substrate displays kinetic constants not unlike those seen with other favored $P_1$ residues. The $k_{cat}/K_M$ for the hydrolysis of protein protease inhibitors is usually very high, comparing favorably to values found with good substrates; only when $k_{cat}$ and $K_M$ (or $K_i$) are examined individually is it seen that both are orders of magnitude lower than for a typical substrate (*2*). Accordingly, we consider $k_{cat}$ alone to be a more relevant basis for comparison when considering the relative vulnerabilities to proteolysis of the spectrum of substrates and inhibitors considered here. The linear peptide representing the CI2 binding loop sequence was cleaved with a kinetic profile placing it among the best of subtilisin peptide substrates, with regard to both $k_{cat}$ and $K_M$. The cyclic peptide was also a good substrate of subtilisin; this finding initially surprised us, because it so clearly contradicts the earlier report by Leatherbarrow and Salacinski (*7*). However, a survey of the literature revealed that we were not the first to find discrepancies with the original report; a third group has also recently synthesized the disulfide-constrained peptide and found it to be a substrate and very poor inhibitor of elastase, rather than the picomolar inhibitor originally reported (*22*).

By comparison with the linear peptide, the cyclic peptide features a $K_M$ decreased by 2 orders of magnitude and a $k_{cat}$ decreased by 1 order of magnitude. In order for a peptide substrate to bind productively to subtilisin, it must adopt the characteristic backbone conformation observed in the reactive-site loop of CI2 and other protease inhibitors, a conformation that is complementary to the enzyme active site. One effect of cyclization is to decrease the accessible conformational space available to the peptide, thereby increasing the proportion of molecules found in a CI2-like conformation, capable of readily combining with the enzyme. As a result, there is less entropic cost associated with binding, and a lower $K_M$ is observed. The explanation for the shift in $k_{cat}$ is perhaps less obvious. The linear and cyclic peptides share identical sequence with CI2 throughout the region of the binding loop and thus should make the same contacts with the enzyme and share a favorable orientation for acylation. The linear peptide is most likely cleaved with rate-determining acylation, like other ordinary peptide substrates of subtilisin (*23*, *26*). CI2, by contrast, forms an acyl−enzyme intermediate rapidly, but retention of the cleaved peptide in the active site dramatically slows the subsequent deacylation step and favors religation of the cleaved peptide bond (*6*). The intermediate $k_{cat}$ value observed with the cyclic

Table 1: Kinetic Constants for Hydrolysis of Different Classes of Substrates by Subtilisin

| substrate | $k_{cat}$ ($s^{-1}$) | $K_M$ (or $K_i$) (M) | $k_{cat}/K_M$ ($M^{-1}s^{-1}$) | note |
|---|---|---|---|---|
| **Esters** | | | | |
| Ac-Ala-Ala-Phe-OMe | 297 | $3.2 \times 10^{-4}$ | $9.4 \times 10^5$ | *a* |
| Z-Gly-Pro-Phe-OEt | 460 | $2 \times 10^{-4}$ | $2.3 \times 10^6$ | *b* |
| **Activated Amides** | | | | |
| suc-Ala-Ala-Pro-Phe-pNA | 50 | $2.7 \times 10^{-4}$ | $1.9 \times 10^5$ | *c* |
| suc-Ala-Ala-Pro-Met-pNA | 13 | $9.0 \times 10^{-5}$ | $1.4 \times 10^5$ | *c* |
| **Peptides** | | | | |
| Z-Gly-Pro-Phe-Gly-Leu | 21 | $6 \times 10^{-4}$ | $3.5 \times 10^4$ | *b* |
| Z-Gly-Pro-Phe-Gly-Gly | 23 | $3.7 \times 10^{-3}$ | $6.3 \times 10^3$ | *b* |
| **Proteins** | | | | |
| casein | 7.2 | $1 \times 10^{-5}$ | $7 \times 10^5$ | *d* |
| clupein sulfate | 45 | $8 \times 10^{-4}$ | $6 \times 10^4$ | *d* |
| **CI2 Derivatives** | | | | |
| linear peptide | 35 | $1.9 \times 10^{-4}$ | $1.8 \times 10^5$ | *e* |
| cyclic peptide | 2.6 | $2.5 \times 10^{-6}$ | $1.0 \times 10^6$ | *e* |
| G83Δ-CI2 | $4.0 \times 10^{-3}$ | $3.4 \times 10^{-9}$ | $1.2 \times 10^6$ | *e* |
| CI2 | $3.8 \times 10^{-6}$ | $2.9 \times 10^{-12}$ | $1.3 \times 10^6$ | *e* |

[a] References *23*, *24*. [b] References *23*, *25*. Note that the constants for Z-Gly-Pro-Phe-Gly-Gly are incorrectly transcribed in ref *23*; these values are taken from the original report (*25*). [c] Determined in our laboratory under our standard assay conditions, these values are in reasonable agreement with various previous reports. [d] Reference *23* and references therein. [e] This work.

peptide suggests that, while it more closely resembles the linear peptide in behaving like a substrate, it may display an altered kinetic profile, with rate-limiting deacylation like CI2. However, if the cyclic peptide were maintained in a stable conformation resembling the binding loop of CI2, one would expect much slower deacylation. Several examples exist in the literature of cyclic peptides that are good inhibitors with resistance to proteolysis, including a 14-amino acid trypsin inhibitor from sunflower (*27*) and an 11-amino acid elastase inhibitor based on the Bowman−Birk inhibitor (*28*). Despite their small size, these peptides are both highly structured in solution, maintaining the characteristic backbone conformation typical of inhibitor binding loops (*29*, *30*). The 18-amino acid cyclic peptide studied here is cleaved nearly 6 orders of magnitude more rapidly than CI2; from this, we conclude that it likely does not exist in a stable CI2-like conformation. To the extent that it assumes the conformation of the CI2 loop, it does so only transiently.

It is notable and somewhat surprising that the CI2 Met-59−Glu-60 bond is specifically targeted for proteolysis by subtilisin in both the linear and cyclic peptides. Although peptide substrates and inhibitors make nearly identical contacts with the protease, the determinants of specificity for substrates and inhibitors are not identical. Proteases interact with substrates or inhibitors predominantly through main-chain−main-chain contacts (*31*). Whereas a substrate main chain is not preconfigured for optimal contact and binds through an induced-fit process (*32*), an inhibitor achieves higher affinity by preorganizing the binding loop into an ideal configuration for lock-and-key recognition by the protease (*1*, *32*). Consequently, substrate specificity is driven by favorable contacts between substrate side chains and complementary enzyme subsites, most significantly between the $P_1$ primary specificity residue of the substrate and the corresponding $S_1$ subsite of the enzyme (*33*). By contrast, inhibitors have been described as "molecular vises": they deliver the same $P_1$ residue to the $S_1$ subsite of any enzyme, regardless of whether the resulting interaction is favorable, neutral, or locally deleterious (*34*−*36*). In the case examined here, while Met-59 is the obligate $P_1$ residue in CI2, it is but one of several potentially favorable $P_1$ residues in the analogous linear and cyclic peptide substrates. Subtilisin typically shows a greater preference for Phe or Tyr at the $P_1$ position (*33*, *37*, *38*); it was therefore surprising when both peptides were cleaved with clear specificity for Met-59, with only trace levels of products representing cleavage after Tyr-61 or any of the other hydrophobic residues present. Our finding demonstrates that the reactive-site sequence of a protein protease inhibitor, which is extremely resistant to proteolysis in the context of the intact inhibitor, is (at least in this case) the preferred site of cleavage in the absence of the inhibitor structure. The observed specificity further suggests that the sequences immediately flanking inhibitor reactive sites may play a greater role than previously appreciated in driving the conformational equilibrium toward the idealized binding conformation.

The synthetic cyclic peptide eliminates the hydrophobic core of CI2, which constrains residues 64−70 in a $\beta$-sheet, and also eliminates the C-terminal glycine residue, which is involved in several electrostatic interactions that affect the binding loop. Gly-83 forms a salt bridge with Arg-65, positioning the arginine side chain to make cross-loop contacts with Glu-60. Gly-83 also accepts a hydrogen bond from the amide nitrogen of Arg-62, stabilizing the tight turn that connects the binding loop to the $\beta$-sheet. The G83Δ-CI2 mutant allows us to dissect the electrostatic effects of Gly-83 from the general stabilizing role of the hydrophobic core. We found G83Δ-CI2 to be cleaved more rapidly than CI2 by 3 orders of magnitude, while the cyclic peptide, lacking both the electrostatic interactions of Gly-83 and the stabilizing influences of the hydrophobic core, was cleaved more rapidly than CI2 by nearly 6 orders of magnitude. It is clear that both the hydrophobic core and the C-terminal Gly-83 play critical roles in stabilization against proteolysis. The results with G83Δ-CI2 are in qualitative agreement with studies on the highly homologous inhibitor eglin C. A mutant of eglin C with truncation of the C-terminal Gly-70 displayed both a proteolysis rate and dissociation constant increased by 2−3 orders of magnitude when assayed with several subtilisins (*39*).

How does the hydrophobic core influence the stability of the binding loop? The core of CI2 makes no direct contacts with subtilisin and contacts the CI2 binding loop internally only through the side chains of Arg-65, Arg-67, and Gly-83. We suggest that the stabilizing influence of the CI2 core derives from two key roles of the $\beta$-sheet on which the binding loop sits. First, the scaffold of the $\beta$-sheet fixes the two ends of the loop, Gly-54 and Ile-63, at a distance of 22 Å from each other, an optimal distance to promote the characteristic extended conformation of the binding loop. Second, incorporation of the strand comprised of residues 64−70 into the $\beta$-sheet orients the side chains of Arg-65 and Arg-67, ensuring that they are always extended upward toward the binding loop, thus lending stability to the entire hydrogen bonding network. Consequently, the absence of the core in the cyclic peptide is enough to eliminate the inhibitory power of CI2, converting it to a substrate for subtilisin.

## ACKNOWLEDGMENT

We thank Justin Lee for assistance in preparation of G83Δ-CI2, and Karen Lu for assistance with binding studies.

## REFERENCES

1. Bode, W., and Huber, R. (1992) Natural protein proteinase inhibitors and their interaction with proteinases. *Eur. J. Biochem. 204*, 433−451.
2. Laskowski, M., Jr., and Kato, I. (1980) Protein inhibitors of proteinases. *Annu. Rev. Biochem. 49*, 593−626.
3. Svendsen, I., Jonassen, I., Hejgaard, J., and Boisen, S. (1980) Amino acid sequence homology between a serine protease inhibitor from barley and potato I inhibitor. *Carlsberg Res. Commun. 45*, 389−395.
4. Boisen, S., Andersen, C. Y., and Hejgaard, J. (1981) Inhibitors of chymotrypsin and microbial serine proteases in barley grains. *Physiol. Plant. 52*, 167−176.
5. McPhalen, C. A., Svendsen, I., Jonassen, I., and James, M. N. G. (1985) Crystal and molecular structure of chymotrypsin inhibitor 2 from barley seeds in complex with subtilisin Novo. *Proc. Natl. Acad. Sci. U.S.A. 82*, 7242−7246.
6. Radisky, E. S., and Koshland, D. E., Jr. (2002) A clogged gutter mechanism for protease inhibitors. *Proc. Natl. Acad. Sci. U.S.A. 99*, 10316−10321.
7. Leatherbarrow, R. J., and Salacinski, H. J. (1991) Design of a small peptide-based proteinase inhibitor by modeling the active-site region of barley chymotrypsin inhibitor 2. *Biochemistry 30*, 10717−10721.
8. Wells, J. A., Ferrari, E., Henner, D. J., Estell, D. A., and Chen, E. Y. (1983) Cloning, sequencing, and secretion of *Bacillus amyloliquefaciens* subtilisin in *Bacillus subtilis*. *Nucleic Acids Res. 11*, 7911−7925.
9. Yang, M. Y., Ferrari, E., and Henner, D. J. (1984) Cloning of the neutral protease gene of *Bacillus subtilis* and the use of the cloned gene to create an in vitro-derived deletion mutation, *J. Bacteriol. 160*, 15−21.
10. Bott, K. F., and Wilson, G. A. (1967) Development of competence in the *Bacillus subtilis* transformation system. *J. Bacteriol. 94*, 562−570.
11. Wilson, G. A., and Bott, K. F. (1968) Nutritional factors influencing the development of competence in the *Bacillus subtilis* transformation system. *J. Bacteriol. 95*, 1439−1449.
12. Schonbaum, G. R., Zerner, B., and Bender, M. L. (1961) The spectrophotometric determination of the operational normality of an α-chymotrypsin solution. *J. Biol. Chem. 236*, 2930−2935.
13. Bender, M. L., Begué-Cantón, M. L., Blakely, R. L., Brubacher, L. J., Feder, J., Gunter, C. R., Kézdy, F. J., Killheffer, J. V., Jr., Marshall, T. H., Miller, C. G., Roeske, R. W., and Stoops, J. K. (1966) The determination of the concentration of hydrolytic enzyme solutions: α-chymotrypsin, trypsin, papain, elastase, subtilisin, and acetylcholinesterase. *J. Am. Chem. Soc. 88*, 5890−5913.
14. DelMar, E. G., Largman, C., Brodrick, J. W., and Geokas, M. C. (1979) A sensitive new substrate for chymotrypsin. *Anal. Biochem. 99*, 316−320.
15. Laskowski, M., Jr., and Sealock, R. W. (1971) Protein Proteinase Inhibitors—Molecular Aspects. *The Enzymes* 3rd ed., Vol. 3, pp 375−473.
16. Bradford, M. M. (1976) A rapid and sensitive method for the quantitation of microgram quantities of protein utilizing the principle of protein−dye binding. *Anal. Biochem. 72*, 248−254.
17. Longstaff, C., Campbell, A. F., and Fersht, A. R. (1990) Recombinant chymotrypsin inhibitor 2: expression, kinetic analysis of inhibition with α-chymotrypsin and wild-type and mutant subtilisin BPN′, and protein engineering to investigate inhibitory specificity and mechanism. *Biochemistry 29*, 7339−7347.
18. Gattiker, A., Bienvenut, W. V., Bairoch, A., and Gasteiger E. (2002) FindPept, a tool to identify unmatched masses in peptide mass fingerprinting protein identification. *Proteomics 2*, 1435−1444.
19. Cornish-Bowden, A. (1995) *Fundamentals of Enzyme Kinetics*, pp 105−108, Portland Press, London.
20. Braun, N. J., Bodmer, J. L., Virca, G. D., Metz-Virca, G., Maschler, R., Bieth, J. G., and Schnebli, H. P. (1987) Kinetic studies on the interaction of eglin *c* with human leukocyte elastase and cathepsin G. *Biol. Chem. Hoppe-Seyler 368*, 299−308.
21. Jackson, S. E., and Fersht, A. R. (1994) Contribution of residues in the reactive site loop of chymotrypsin inhibitor 2 to protein stability and activity. *Biochemistry 33*, 13880−13887.
22. Gururaja, T. L., Narasimhamurthy, S., Payan, D. G., and Anderson, D. C. (2000) A novel artificial loop scaffold for the noncovalent constraint of peptides. *Chem. Biol. 7*, 515−527.
23. Philipp, M., and Bender, M. L. (1983) Kinetics of subtilisin and thiolsubtilisin. *Mol. Cell. Biochem. 51*, 5−32.
24. Morihara, K., Oka, T., and Tsuzuki, H. (1974) Comparative study of various serine alkaline proteinases from microorganisms. *Arch. Biochem. Biophys. 165*, 72−79.
25. Morihara, K., and Oka, T. (1977) A kinetic investigation of subsites $S_1'$ and $S_2'$ in α-chymotrypsin and subtilisin BPN′. *Arch. Biochem. Biophys. 178*, 188−194.
26. Wells, J. A., Cunningham, B. C., Graycar, T. P., and Estell, D. A. (1986) Importance of hydrogen-bond formation in stabilizing the transition state of subtilisin. *Philos. Trans. R. Soc. London A 317*, 415−423.
27. Luckett, S., Garcia, R. S., Barker, J. J., Konarev, Al. V., Shewry, P. R., Clarke, A. R., and Brady, R. L. (1999) High-resolution structure of a potent, cyclic proteinase inhibitor from sunflower seeds. *J. Mol. Biol. 290*, 525−533.
28. McBride, J. D., Freeman, H. N. M., and Leatherbarrow, R. J. (1999) Selection of human elastase inhibitors from a conformationally constrained combinatorial peptide library. *Eur. J. Biochem. 266*, 403−412.
29. Korsinczky, M. L. J., Schirra, H. J., Rosengren, K. J., West, J., Condie, B. A., Otvos, L., Anderson, M. A., and Craik, D. J. (2001) Solution structures by $^1$H NMR of the novel cyclic trypsin inhibitor SFTI-1 from sunflower seeds and an acyclic permutant. *J. Mol. Biol. 311*, 579−591.
30. Brauer, A. B. E., Kelly, G., McBride, J. D., Cooke, R. M., Matthews, S. J., and Leatherbarrow, R. J. (2001) The Bowman−Birk inhibitor reactive site loop sequence represents an independent structural β-hairpin motif. *J. Mol. Biol. 306*, 799−807.
31. Jackson, R. M. (1999) Comparison of protein−protein interactions in serine protease-inhibitor and antibody−antigen complexes: Implications for the protein docking problem. *Protein Sci. 8*, 603−613.
32. Hubbard, S. J., Campbell, S. F., and Thornton, J. M. (1991) Molecular recognition. Conformational analysis of limited proteolytic sites and serine proteinase protein inhibitors. *J. Mol. Biol. 220*, 507−530.
33. Perona, J. J., and Craik, C. S. (1995) Structural basis of substrate specificity in the serine proteases. *Protein Sci. 4*, 337−360.
34. Qasim, M. A., Ganz, P. J., Saunders, C. W., Bateman, K. S., James, M. N. G., and Laskowski, M., Jr. (1997) Interscaffolding additivity. Association of $P_1$ variants of eglin c and turkey ovomucoid third domain with serine proteases. *Biochemistry 36*, 1598−1607.
35. Lu, W., Apostol, I., Qasim, M. A., Warne, N., Wynn, R., Zhang, W. L., Anderson, S., Chiang, Y. W., Ogin, E., Rothberg, I., Ryan, K., and Laskowski, M., Jr. (1997) Binding of amino acid side-chains to $S_1$ cavities of serine proteinases. *J. Mol. Biol. 266*, 441−461.
36. Laskowski, M., Jr., and Qasim, M. A. (2000) What can the structures of enzyme−inhibitor complexes tell us about the structures of enzyme substrate complexes? *Biochim. Biophys. Acta 1477*, 324−337.
37. Estell, D. A., Graycar, T. P., Miller, J. V., Powers, D. B., Burnier, J. P., Ng, P. G., and Wells, J. A. (1986) Probing steric and hydrophobic effects on enzyme−substrate interactions by protein engineering. *Science 233*, 659−663.
38. Wells, J. A., Cunningham, B. C., Graycar, T. P., and Estell, D. A. (1987) Recruitment of substrate-specificity properties from one enzyme into a related one by protein engineering. *Proc. Natl. Acad. Sci. U.S.A. 84*, 5167−5171.
39. Lu, W.-Y., Starovasnik, M. A., Dwyer, J. J., Kossiakoff, A. A., Kent, S. B. H., and Lu, W. (2000) Deciphering the role of the electrostatic interactions involving Gly70 in eglin *c* by total chemical protein synthesis. *Biochemistry 39*, 3575−3584.

BI034275D